

 Open access • Journal Article • DOI:10.1088/1361-6463/AB78D3

## Stored energy of arbitrary metamaterial inclusions — Source link

Ozuem Chukwuka, Divitha Seetharamdoo, M. Hassanein Rabah

**Institutions:** IFSTTAR, university of lille

**Published on:** 03 Apr 2020 - Journal of Physics D (IOP Publishing)

**Topics:** Metamaterial antenna, Metamaterial and Modal

Related papers:

- [Simulation of Electromagnetic Fields in Double Negative Metamaterials](#)
- [Modeling Optical Metamaterials with Strong Spatial Dispersion](#)
- [Reflection and transmission of light at periodic layered metamaterial films](#)
- [Beyond local effective material properties for metamaterials](#)
- [Electromagnetic parameter retrieval from inhomogeneous metamaterials](#)

Share this paper:    

View more about this paper here: <https://typeset.io/papers/stored-energy-of-arbitrary-metamaterial-inclusions-3yrzp8ub6k>



**HAL**  
open science

## Stored energy of arbitrary metamaterial inclusions

Ozuem Chukwuka, Divitha Seetharamdoo, Mhamad-Hassanein Rabah

► **To cite this version:**

Ozuem Chukwuka, Divitha Seetharamdoo, Mhamad-Hassanein Rabah. Stored energy of arbitrary metamaterial inclusions. *Journal of Physics D: Applied Physics*, IOP Publishing, 2020, 23 (53), pp.235501. 10.1088/1361-6463/ab78d3 . hal-02925012

**HAL Id: hal-02925012**

**<https://hal.archives-ouvertes.fr/hal-02925012>**

Submitted on 28 Aug 2020

**HAL** is a multi-disciplinary open access archive for the deposit and dissemination of scientific research documents, whether they are published or not. The documents may come from teaching and research institutions in France or abroad, or from public or private research centers.

L'archive ouverte pluridisciplinaire **HAL**, est destinée au dépôt et à la diffusion de documents scientifiques de niveau recherche, publiés ou non, émanant des établissements d'enseignement et de recherche français ou étrangers, des laboratoires publics ou privés.

# Stored energy of arbitrary metamaterial inclusions

Ozuem Chukwuka,<sup>a)</sup> Divitha Seetharamdo, <sup>b)</sup> and M. Hassanein Rabah  
*Univ. Lille Nord de France, IFSTTAR, COSYS, LEOST F-59650 Villeneuve d'Ascq, France.*

(Dated: 24 July 2020)

5 Electromagnetic metamaterials are generally defined and classified in terms of their effective  
 parameters. They are evaluated in the far-field which limits the evaluation of its near field  
 interaction in some applications such as metamaterial inspired design. An alternative ap-  
 10 proach proposed in this paper is based on the modal stored energy of metamaterial inclusion.  
 This approach is based on the surface current distribution which would address the challenge  
 of metamaterial near-field application. This paper describes a method for quantifying the  
 modal stored energy of arbitrary-shaped metamaterial inclusions based on the theory of char-  
 15 acteristic modes. The theory of characteristic modes is independent of excitation, gives good  
 physical insight into the behaviour of an inclusion and would be helpful for near-field applica-  
 tion of metamaterials. The modal stored energy approach is also compared with the common  
 effective parameter approach. It shows similarity in terms of the physical and qualitative  
 analysis when far-field assumptions are accounted for. The broadside-coupled split-ring res-  
 onator and the S-shaped inclusion are considered. The physical and qualitative analysis based  
 on the modal stored energy approach shows a good agreement with the effective parameter  
 approach.

20 Keywords: Stored energy, metamaterial antenna, modal stored energy, metamaterial, effec-  
 tive parameter.

## I. INTRODUCTION

55 Electromagnetic systems such as antennas are char-  
 25 acterised by the way in which they dissipate, store and  
 radiate electromagnetic energy. These quantities are use-  
 ful for understanding the physics, design application and  
 evaluation of the radiation performances such as the ra-  
 30 diation efficiency and performance bounds<sup>1-4</sup>. It is gen-  
 erally suggested that electromagnetic artificial materi-  
 als such as metamaterial can improve radiating perfor-  
 mances in several configurations<sup>5</sup>. These metamaterials  
 (MTMs) are defined in terms of their effective material  
 65 parameters i.e. permeability  $\mu$  and permittivity  $\varepsilon$  func-  
 tions and always need to be extracted<sup>6</sup> from their far-  
 35 field quantity. Importantly, an interesting phenomena for  
 electromagnetic systems application happen at the region  
 of resonance<sup>7,8</sup> where effective parameters are not always  
 valid. Hence, with the growing near-field applications of  
 40 MTM to electromagnetic systems like antenna<sup>9,10</sup>, it is  
 interesting to analyze MTM around its region of reso-  
 nance using similar quantities of most electromagnetic  
 systems. Unlike effective parameters which are valid in  
 far-field, stored energy quantities define near-field inter-  
 45 action of electromagnetic systems<sup>11</sup>. Although, there are  
 existing methods for evaluating electromagnetic energy  
 such as the scattering approach given in terms of the  
 conduction or polarization current<sup>12</sup>, a more robust and  
 intuitive approach is the method of moments<sup>13</sup>.

50 The method of moments which is applied in the the-  
 ory of characteristic modes (TCM) brings physical insight  
 through intuitive knowledge into the electromagnetic en-  
 ergy of radiating structures using a modal approach<sup>14</sup>.

It expands current as a number of basis function and  
 green function and by solving the derived impedance  
 matrix as a generalized eigenvalue equation, electromag-  
 netic energy can be calculated for any external excit-  
 ing field. In other words, the application of theory of  
 characteristic modes is independent of excitation, ap-  
 60 plicable to arbitrary-shaped structures, takes into ac-  
 count the nature of the material and requires only few  
 modes to describe the global behaviour of electrically  
 small structures<sup>14</sup>. Thus, TCM is popular for the de-  
 sign of many electromagnetic systems especially antenna  
 design<sup>15-18</sup> for various applications. In previous work,  
 the theory of characteristic modes was extended to de-  
 sign MTM inclusion<sup>19</sup>. It was shown that one of the  
 challenges with these inclusions especially magnetic in-  
 65 clusion is that its magnetic properties are exhibited when  
 excitation is placed in a specific polarization. Thus, it is  
 important to consider excitation and polarization effect  
 in describing the modal stored energy of MTM inclusion.

The modal stored energy approach for metamaterial  
 inclusion is useful for selecting an inclusion to associate  
 with an electromagnetic system like antenna. Already,  
 many electromagnetic designs make use of modal ap-  
 70 proach such as evaluation of antenna Q-factor<sup>20-22</sup>, selec-  
 tion of antenna excitation source<sup>23</sup>, design of metamate-  
 rial inclusion for antenna application<sup>24-27</sup> and the study  
 of electromagnetic structures<sup>28-30</sup>. This is due to the  
 numerous advantages which include its independence of  
 excitation source, applicability to arbitrary-shaped struc-  
 75 tures and the physical insight it brings into the behaviour  
 of radiating structures<sup>14,15</sup>. The design of metamaterial,  
 antenna and electromagnetic devices can therefore be an-

85 analyzed using similar modal quantities while leveraging on the physical insight and other advantages of modal analysis approach.

This paper shows a method to quantitatively evaluate the modal stored energy of MTM inclusions using TCM. 90 TCM is independent of excitation and only takes into account the properties and structure of the material. The methodology is applied to MTM inclusions with known effective parameter quantity. In order to provide a qualitative appreciation by comparison to common effective 95 parameters, new steps are introduced to the modal stored energy approach to account for the polarization and excitation dependence of MTM inclusions. Two elementary structures, broadside-coupled split-ring resonator (BC-SRR) and S-shaped unit cell are considered to demonstrate our approach. The commercial method of moment (MoM) based characteristic modes analysis tool (FEKO)<sup>31</sup> is used to evaluate the eigenvalue, modal surface current distribution and modal weighting coefficient. The impedance matrix is extracted and used to evaluate 105 the stored energy.

## II. FORMULATION FOR MODAL STORED ENERGY EVALUATION BASED ON THEORY OF CHARACTERISTIC MODES

The modal stored energy formulation is based on the Theory of Characteristic Modes (TCM) which represents 130 a structure in terms of its surface impedance  $Z^{14}$ . The surface impedance  $Z$  is given as:

$$Z = R + jX, \quad (1)$$

where  $R$  is the real part and  $X$  is the imaginary part of the impedance. Using the derived impedance  $Z$ , a solution is found for the generalized eigenvalue equation given in equation (2) as:

$$[X][I] = \lambda_n[R][I], \quad (2)$$

110 where  $\lambda_n$  is the eigenvalue of each  $n$  mode and  $I$  is the eigen-current.

Although this paper uses TCM based method for the presented formulation of the modal stored energy, TCM is not explicitly dealt here and can be found in the literature<sup>14,15,32,33</sup>. The value of  $\lambda_n$  is directly related to the nature of the modal stored energy by the imaginary part of the impedance matrix  $X$  with  $\lambda_n$  greater than zero indicating a stored magnetic energy,  $\lambda_n$  less than zero indicating a stored electric energy and  $\lambda_n$  equal to zero indicating that both the magnetic energy and electric energy are of equal magnitude which results in total radiation with no stored energy<sup>2,15,34</sup>. This modal stored energy deductions are however only qualitative<sup>14</sup>. On the other hand, modal quantitative stored energy value of MTM inclusion provides a new way to reliably analyze 120 artificial materials. This would aid their choice for specific applications especially in cases where the near-field behaviour needs to be predicted such as its association to antennas<sup>10</sup> and sensors.

Using the surface impedance  $Z$  derived from TCM, the modal stored energy operator ( $W_{sto}$ ) derived in<sup>35,36</sup> and as applied to antenna design<sup>2</sup> is:

$$W_{sto} = W_m + W_e = \frac{1}{4\omega} I^H X' I, \quad (3)$$

where  $\omega$  is the angular frequency,  $I$  is the eigen-current from the generalized eigenvalue equation,  $I^H$  is the Hermitian transpose of the eigen-current and  $X'$  is given in<sup>2</sup> as equation (4):

$$X' = \omega \frac{\partial X}{\partial \omega}. \quad (4)$$

Separating  $W_{sto}$  into electric energy ( $W_e$ ) and magnetic energy ( $W_m$ ) component<sup>2</sup>, we have equation (5) and (6):

$$W_m = \frac{1}{8\omega} I^H X_m I, \quad (5)$$

and

$$W_e = \frac{1}{8\omega} I^H X_e I, \quad (6)$$

where,

$$X_m = X' + X, \quad (7)$$

and

$$X_e = X' - X. \quad (8)$$

$X$  being a 3D matrix complicates the implementation of  $X'$ , thus further simplification is carried out by splitting the impedance  $Z$  into its inductive and capacitive component as:

- For  $X$  as an inductive impedance:

$$X = \omega L, \quad (9)$$

differentiating both sides with respect to  $\omega$ ,

$$\frac{\partial X}{\partial \omega} = L. \quad (10)$$

But from equation (4),

$$X' = \omega \frac{\partial X}{\partial \omega}$$

substituting equation (10) into equation (4),

$$X' = \omega \frac{\partial X}{\partial \omega} = \omega L, \quad (11)$$

therefore substituting equation (9) into equation (11),

$$X' = X. \quad (12)$$

- For  $X$  as a capacitive impedance:

$$X = \frac{-1}{\omega C}, \quad (13)$$

differentiating both sides with respect to  $\omega$ ,

$$\frac{\partial X}{\partial \omega} = \frac{1}{C\omega^2}. \quad (14)$$

But from equation (4),

$$X' = \omega \frac{\partial X}{\partial \omega}$$

substituting equation (14) into equation (4),

$$X' = \omega \frac{\partial X}{\partial \omega} = \omega \frac{1}{C\omega^2} = \frac{1}{C\omega}, \quad (15)$$

therefore substituting equation (13) into equation (15),

$$X' = -X. \quad (16)$$

135 The conclusion therefore is that  $X'$  equals  $|X|$  and the two possible analytical solution for  $X'$  depends on the nature of  $W_{sto}$  as either electric or magnetic. This conclusion has been qualitatively concluded using the first derivative of  $\lambda_n$  with respect to the frequency<sup>21</sup>.

140 To ensure uniformity of the modal stored energy value, just as it is done for  $W_{sto}$  in antenna applications for evaluation of Q-factor,  $W_m$  and  $W_e$  are normalized with respect to the radiated power ( $P_r$ )<sup>2,20,37</sup> in equation (17):

$$P_r = I^H R I. \quad (17)$$

### 145 III. EVALUATION AND ANALYSIS OF MODAL STORED ENERGY OF MTM INCLUSION

In this section, the  $W_{sto}$  formulation is applied to MTM inclusions to determine their modal magnetic and electric energies. The difference between the magnetic and electric energy ( $W_m - W_e$ ) is used to determine the dominant energy with zero value indicating a vanishing energy (resonance)<sup>34</sup>. Two elementary inclusions with known effective parameters are considered; the Broadside-Coupled Split-Ring Resonator (BC-SRR) and the S-shaped inclusion. While the BC-SRR is a well known and extensively studied magnetic MTM inclusion, 155 the S-shaped inclusion exhibit both the electric and magnetic behaviour at different resonant frequencies. The analysis for the structures are done in the frequency range of 1 GHz to 4 GHz to cover the resonance of both inclusions. 160

#### III.A. Broadside-Coupled Split-Ring Resonator (BCSRR)

The BC-SRR which is known to exhibit artificial magnetism is made up of two circular symmetric loops of PEC material and placed on the two opposite sides of a teflon substrate of effective permittivity,  $\epsilon_r$  2.2. It resonate at 2.35 GHz and its dimension is given in figure 1.

170 The artificial magnetic behavior of this BC-SRR was shown by Rabah et al.<sup>19</sup> using characteristic modes and static polarizability. The TCM commercial software was used for the modal analysis of the structure to solve the generalized eigenvalue equation and the obtained result of the TCM analysis for the structure is represented by

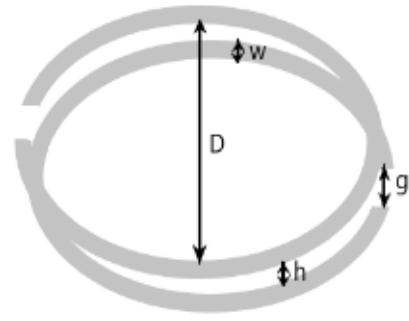
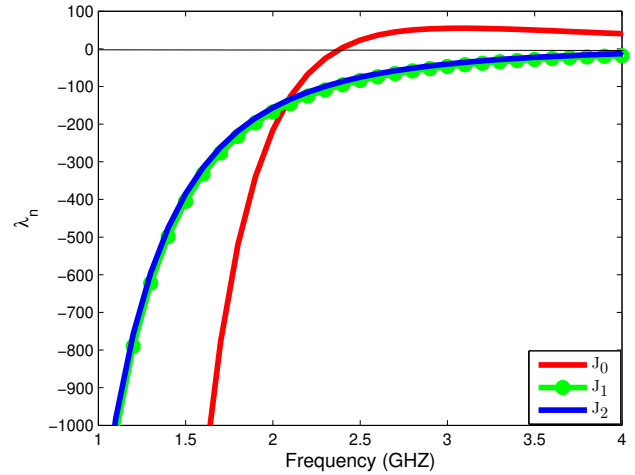
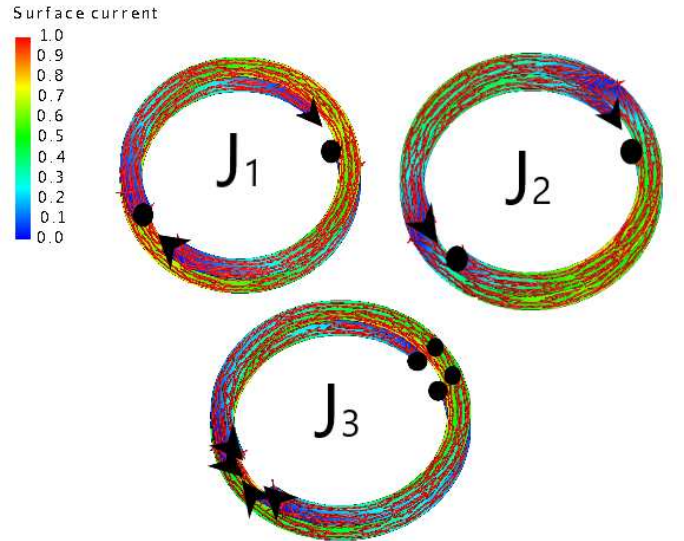


FIG. 1: BC-SRR with dimensions:  $D = 11.25$  mm,  $W = 1$  mm,  $g = 1.95$  mm,  $h =$  substrate height  $= 1.08$  mm.



(a)



(b)

FIG. 2: BC-SRR inclusion: (a)eigenvalue ( $\lambda_n$ ) with respect to frequency (b)surface current distribution

the plot of  $\lambda_n$  with respect to frequency in figure 2a and the surface current distribution in figure 2b.

Only the fundamental mode  $J_0$  in red cross the zero mark at 2.35 GHz as shown in figure 2a hence, only one resonance occur. The  $W_e$  and  $W_m$  are of equal magnitude and no energy is stored at this frequency of 2.35 GHz. Also, this resonance frequency of 2.35 GHz is close to that of the BC-SRR analyzed by Rabah et al.<sup>19</sup> which was referred to as the fundamental DC mode of a circular loop. The other modes  $J_1$  and  $J_2$  in green and blue have negative values of  $\lambda_n$  through out the considered frequency band and indicates that they store more  $W_e$ . From the current profile shown in figure 2b, the black arrow head show the direction of the current flow, the black dot show the starting point of the current flow. The behaviour of the modes can be easily described as magnetic or electric.  $J_0$  show a magnetic current distribution with both loops having similar direction of current flow while  $J_1$  and  $J_2$  show a current distribution pattern similar to that of an electric dipole with the current flowing in the opposite direction on both loops.

To quantify the energies with respect to frequency for each mode, the impedance matrix is extracted from the commercial software and the  $W_{sto}$  formulation of section II is applied to determine the modal magnetic and electric energies. The result of the dominant energy is represented by the normalized  $(W_m - W_e)$  with respect to frequency in figure 3.

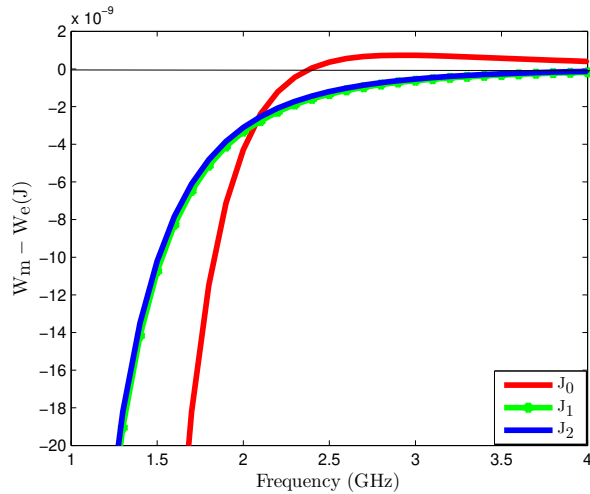


FIG. 3: Normalized  $(W_m - W_e)$  with respect to frequency of BC-SRR.

The value of  $W_e$  and  $W_m$  are equal at 2.35 GHz for mode  $J_0$  in red thus, the value of normalized  $(W_m - W_e)$  is 0 J at this frequency.  $J_1$  and  $J_2$  in green and blue both have negative values of  $(W_m - W_e)$  within the considered frequency band and implies that  $W_e$  remains greater than  $W_m$ . The  $(W_m - W_e)$  quantity agrees with the qualitative deductions of the eigenvalue ( $\lambda_n$ ) curve.

### III.B. S-shaped MTM inclusion

The S-shaped inclusion exhibit both the electric and magnetic behaviour due to its bianisotropic character<sup>38</sup>. It is made of a PEC sheet forming an S-shape and its dimensions are shown in figure 4.

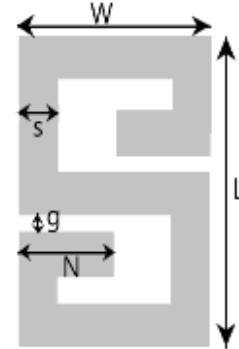


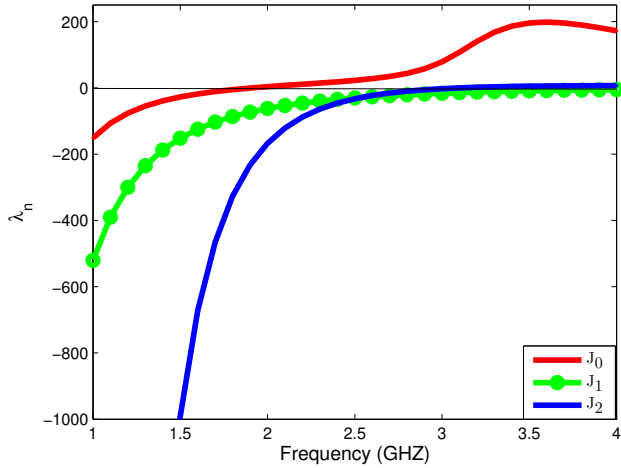
FIG. 4: S-shaped inclusion with dimensions:  $L = 27$  mm,  $W = 13$  mm,  $g = 1.1$  mm,  $N = 4$  mm,  $s = 1.5$  mm.

The S-shaped structure has its fundamental resonance at 1.92 GHz. The same analysis followed for the BC-SRR inclusion was carried out for the S-shaped inclusion. The TCM commercial software was used for the modal analysis of the structure and the obtained result of the TCM analysis is represented by the plot of  $\lambda_n$  with respect to frequency in figure 5a and the surface current distribution in figure 5b.

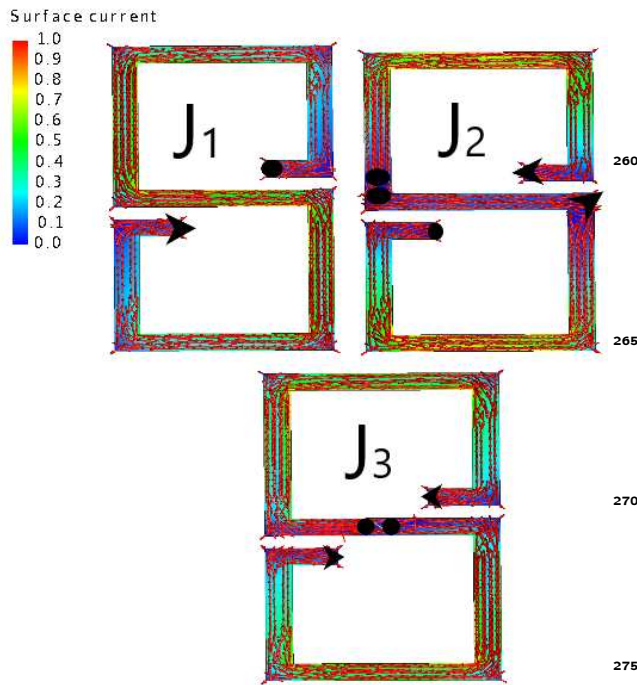
$J_0$  and  $J_2$  of figure 5a in red and blue cross the zero mark at 1.92 GHz and 3.1 GHz respectively. This corresponds to the resonance frequencies and indicates that  $W_e$  and  $W_m$  are of equal magnitude at these frequencies and no modal stored energy.  $J_1$  on the other hand remains with negative values of  $\lambda_n$  with respect to the considered frequency band implying that  $W_e$  is dominant. The behaviour of the modes as electric or magnetic can also be analyzed using the surface current distribution in figure 5b. The black arrow head show the direction of the current flow and the black dot shows its starting point. The current distribution of  $J_0$  is similar to that of an electric dipole with the current flowing in one direction.  $J_1$  also show an electric dipole current distribution splitted into two halves with the current flowing in opposite directions on the two halves.  $J_2$  show a magnetic current distribution with the current flowing in the same direction when the S-shape is split into two equal halves.

To quantify the modal energies with respect to frequency for each mode, the impedance matrix is extracted from the commercial software and the  $W_{sto}$  formulation of section II is applied to determine the modal magnetic and electric energies. The result of the dominant energy is represented by the normalized  $(W_m - W_e)$  with respect to frequency in figure 6.

$J_0$  and  $J_2$  of figure 6 in red and blue show that at the resonance frequency of 1.92 GHz and 3.1 GHz respectively,  $(W_e - W_m)$  is 0 J and the magnitude of  $W_m$  and



(a)



(b)

FIG. 5: S-shaped inclusion: (a)eigenvalue  $\lambda_n$  with respect to frequency (b)surface current distribution

$W_e$  are of the same value. The region of the curve that lies in the negative part indicates that  $W_e$  is dominant while the region in the positive part indicates that  $W_m$  is dominant.  $J_1$  in green has negative values across the considered frequency band hence,  $W_e$  is dominant across the considered frequency band. The  $(W_m - W_e)$  quantity agrees with the qualitative deductions of the eigenvalue ( $\lambda_n$ ) curve.

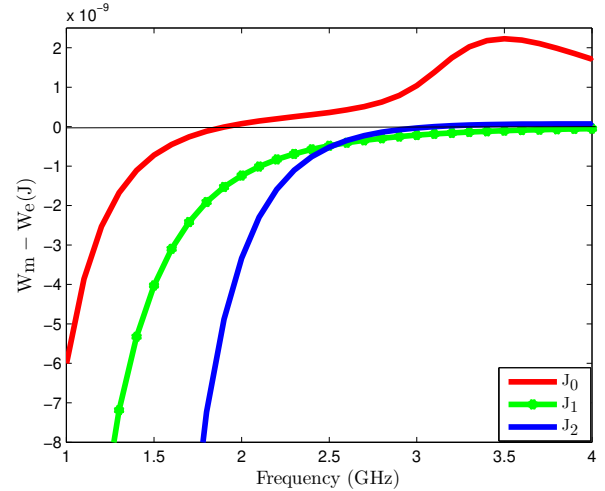


FIG. 6: Normalized  $(W_m - W_e)$  with respect to frequency of S-shaped inclusion.

#### IV. COMPARISON BETWEEN STORED ENERGY AND EFFECTIVE PARAMETERS OF MTM INCLUSION

Generally, the physical behaviour of MTM are described in terms of effective parameters<sup>39–42</sup>. The later are calculated from far-field complex reflection and transmission coefficient<sup>41,42</sup> using classical approach of extraction techniques<sup>40,43,44</sup>. The effective parameters of MTM structures are represented as the permittivity  $\epsilon$  and permeability  $\mu$  values which describes them as electric or magnetic MTM<sup>45</sup>. If this provides physical insight, the association of MTM to devices at microwave frequencies in the near-field region such as for antenna and sensor designs<sup>46–48</sup> can not be studied in a reliable manner based on effective parameters.

Modal stored energy on the other hand is a quantity derived from modal current and account for near-field effects<sup>1</sup>. It permits studying the behaviour of shapes separately from its feeding structure. This means that the modal quantities of the structure is calculated once while the effect of the feeding can be superimposed<sup>20,49</sup>. The modal stored energy being quantitative and independent of excitation is believed to be a more reliable analysis of MTM since the properties of MTM are based on their shapes<sup>50</sup>.

In this section, we present a comparison between the effective parameter and the dominant stored energy such that within a given frequency band, one can appreciate the convergence in terms of physical and qualitative analysis. Most inclusions especially magnetic inclusion have their magnetic properties exhibited when excitation is placed in a specific polarization<sup>19</sup>. The TCM based energies  $W_m$  and  $W_e$  are excitation and polarization independent whereas, the effective parameters are excitation and polarization dependent. To enable a comparison between the two approach, new steps are introduced to the

295 calculation of the differential stored energies (i.e.  $W_m$   
 -  $W_e$ ) to account for the polarizability of the inclusions.  
 Additional steps are introduced to the calculation of ( $W_m$   
 -  $W_e$ ) in figure 7. 335

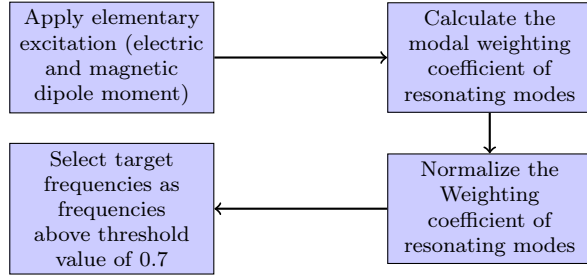


FIG. 7: Additional steps for calculating ( $W_m - W_e$ ).

300 The block diagram in figure 7 describes the procedure  
 to take into account the effect of excitation and polariza-  
 tion in the modal stored energy analysis of MTM inclu-  
 sion. First, an elementary excitation (electric and mag-  
 netic dipole moment) is applied to the structure and the  
 modal weighting coefficient  $MWC_n$ <sup>14</sup> is derived from the  
 TCM based commercial software where  $MWC_n$  is given  
 305 as equation (18):

$$MWC_n = \frac{V^i J_n}{1 + j\lambda_n}, \quad (18)_{340}$$

where  $V^i$  is the applied excitation,  $\lambda_n$  is the eigenvalue  
 and  $J_n$  is the surface current of the  $n^{th}$  mode.

310 The  $MWC_n$  give information of the modal response  
 to the applied excitation. The  $MWC_n$  of the resonant  
 modes are normalized with their maximum value. Stored  
 energy is related to bandwidth by Q-factor definition<sup>51,52</sup>  
 hence, we evaluate the modal half power bandwidth using  
 the TCM bandwidth definition. This represents the  
 315 region of frequencies that participate in radiation and  
 is given as frequencies with a modal significance above  
 0.7<sup>15</sup>. The dominant energy within the modal bandwidth  
 (i.e. having a value above 0.7 of the normalized  $MWC_n$ )  
 are considered and referred to as target frequencies. They  
 320 account for the behaviour before and after the resonance  
 frequencies which are important for electromagnetic appli-  
 cations. To quantitatively describe an inclusion, the  
 dominant energy ( $W_m - W_e$ ) within the target frequen-  
 cies are summed up and the sign of the summation indi-  
 325 cates the dominant energy within the modal bandwidth  
 of the structure. It tells if the inclusion is electric or mag-  
 netic. A positive value, indicates dominant  $W_m$  and the  
 inclusion is magnetic while a negative value, implies that  
 $W_e$  is dominant and the inclusion is electric. 360

330 This procedure is applied to the inclusions whose domi-  
 nant modal energy values ( $W_m - W_e$ ) were evaluated in  
 the previous section. 365

#### IV.A. Broadside Coupled Split Ring Resonator (BCSRR)

The BC-SRR is excited with a magnetic dipole mo-  
 ment and only the resonant mode  $J_0$  is considered. The  
 normalized  $MWC_n$  with respect to frequency extracted  
 from the TCM based simulation software is shown in fig.  
 8.

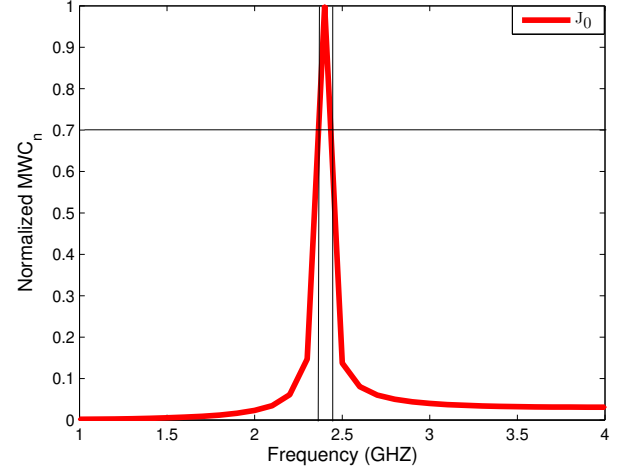


FIG. 8: Normalized  $MWC_n$  with respect to frequency of  
 BC-SRR.

The horizontal thin black line in figure 8 show the  
 threshold value of 0.7 which indicates the region of the  
 target frequencies between 2.35 GHz and 2.43 GHz. The  
 shift of the centre frequency from the resonance is due to  
 the coupling of the excitation with the structure. The  
 summation of the normalized ( $W_m - W_e$ ) at the target  
 frequencies from the previous section for the BC-SRR is  
 $4.1969 \times 10^{-10}$  J. The value is positive hence, one can  
 conclude that  $J_0$  of BC-SRR exhibits a magnetic behav-  
 iour and therefore it is a magnetic inclusion. This analysis  
 agree with the current profile of BC-SRR. In comparison  
 to the classical approach of effective parameters of the  
 BC-SRR, the plot of effective parameters ( $\epsilon$  and  $\mu$ ) with  
 respect to frequency is shown in figure 9.

$\epsilon$  and  $\mu$  in green and red respectively give informa-  
 tion of the dominant property of the BC-SRR. Around  
 the resonance frequency of 2.35 GHz, the values of  $\mu$  are  
 higher than that of  $\epsilon$  and the magnetic behaviour of the  
 structure dominates thus, the inclusion is magnetic. This  
 qualitative description is in agreement with that of the  
 dominant stored energy analysis.

#### IV.B. S-shaped MTM inclusion

The S-shaped inclusion has two resonant modes  $J_0$  and  
 $J_2$  with different behavior. The S-shaped inclusion is ex-  
 cited with an electric dipole moment and the normal-  
 ized  $MWC_n$  with respect to frequency which has been  
 extracted from the TCM based simulation software is  
 shown in figure 10.



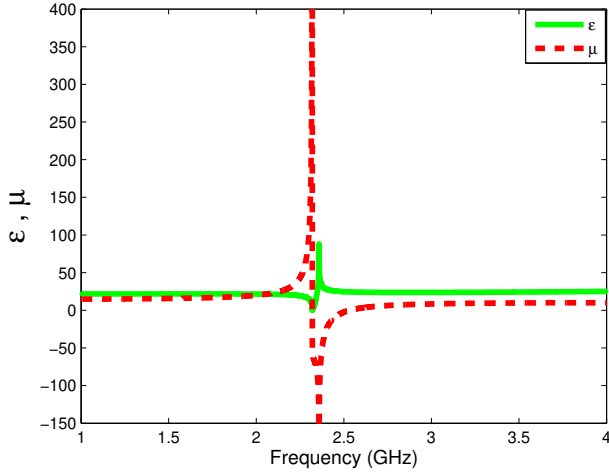


FIG. 9:  $\epsilon$  and  $\mu$  with respect to the frequency of BC-SRR.

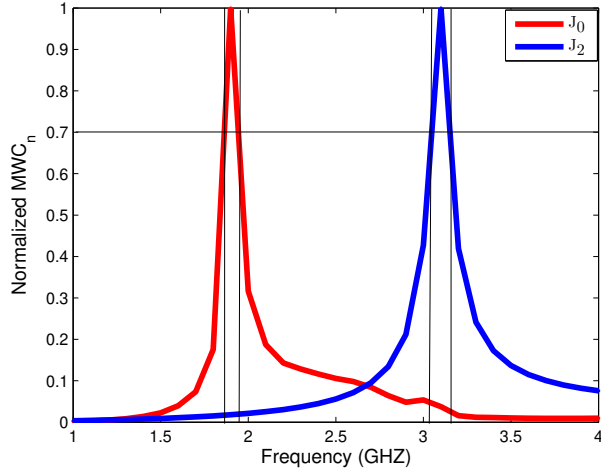


FIG. 10: Normalized  $MWC_n$  with respect to frequency of S-shaped inclusion.

The horizontal thin black line in figure 10 show the threshold value of 0.7 which indicates the region of the target frequencies between 1.86 GHz and 1.94 GHz for mode  $J_0$  in red and between 3.05GHz and 3.2 GHz for mode  $J_2$  in blue. The shift of the centre frequency from the resonance frequency is due to the coupling of the excitation with the structure. The summation of the  $(W_m - W_e)$  values at the target frequencies from the previous section for the S-shaped inclusion is  $-1.2 \times 10^{-10}$  J and  $2.5545 \times 10^{-11}$  J for  $J_0$  and  $J_2$  respectively. The value for  $J_0$  is negative indicating that the inclusion behave as an electric structure around the first resonance.  $J_2$  has a positive value which implies that the inclusion behave as a magnetic structure at its second resonance. This analysis agree with the current profile of the S-shaped inclusion. In comparison to the classical approach of effective parameters of the S-shaped inclusion, the plot of

effective parameters ( $\epsilon$  and  $\mu$ ) with respect to frequency is shown in figure 11.

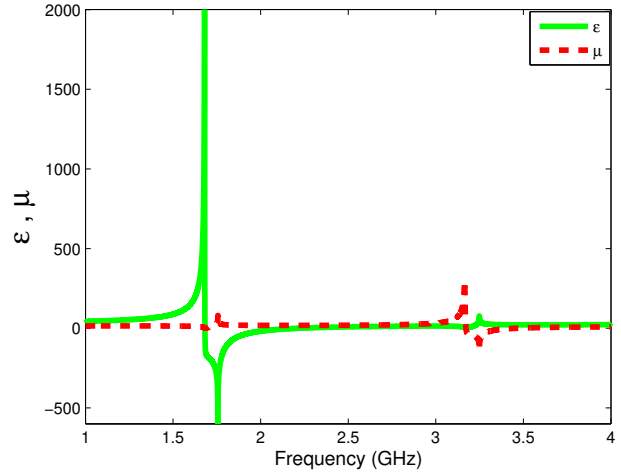


FIG. 11:  $\epsilon$  and  $\mu$  with respect to the frequency of S-shaped inclusion.

$\epsilon$  and  $\mu$  in green and red respectively give information of the dominant property of the S-shaped inclusion. Around the fundamental resonance frequency of 1.92 GHz, the values of  $\epsilon$  are higher than that of  $\mu$  and the electric behaviour dominates the magnetic behaviour hence, the structure behave as an electric inclusion. On the other hand, the values of  $\mu$  are higher than that of  $\epsilon$  at the second resonance of 3.01 GHz and the structure behave as a magnetic inclusion at this frequency. This qualitative description is in agreement with that of the dominant stored energy analysis for the S-shaped inclusion.

## V. CONCLUSION

In comparison to the effective parameters approach of defining metamaterial inclusions which are valid in the far-field region and may not be reliable for near-field analysis and modal design of electromagnetic devices, this paper presents a modal stored energy approach which is based on modal current and account for near-field effects. This method can be applied to any resonant metamaterial structure and it is based on the theory of characteristics modes which is independent of excitation and brings physical insight into the resonant property of a structure. Two elementary inclusions, BC-SRR and S-shaped inclusions were considered for demonstration. Also, a comparison between the effective parameters and the modal stored energy approach is done to show the convergence in terms of physical and qualitative analysis. This comparison is achieved by introducing additional steps into the calculation of modal stored energy to take into account the polarization and excitation dependence of inclusions. Both methods show good agreement in their physical and qualitative analysis. This approach

is useful in the application of modal analysis for design-485  
 ing metamaterial-inspired structures including antenna,  
 sensor and cloaks.

## ACKNOWLEDGMENTS

The authors acknowledge partial funding of this re-  
 search work by the regional project SMARTIES in the  
 framework of the ELSAT 2020 program co-financed by  
 the European Union with the European Regional devel-  
 opment fund, the French state and Hauts de France Re-  
 gional council. One of the author acknowledge funding  
 of IFSTTAR for a PhD scholarship.

a) Electronic mail: ozuem.chukwuka@ifsttar.fr

b) Electronic mail: divitha.seetharamdoo@ifsttar.fr

<sup>1</sup>M. Capek, L. Jelinek, P. Hazdra, and J. Eichler, “The measurable  
 $q$  factor and observable energies of radiating structures,” IEEE  
 Transactions on Antennas and Propagation **62**, 311–318 (2014).

<sup>2</sup>M. Capek and L. Jelinek, “Optimal composition of modal currents  
 for minimal quality factor  $q$ ,” IEEE Transactions on Antennas  
 and Propagation **64**, 5230–5242 (2016).

<sup>3</sup>M. Gustafsson and B. Jonsson, “Stored electromagnetic energy  
 and antenna  $q$ ,” arXiv preprint arXiv:1211.5521 (2013).

<sup>4</sup>M. Gustafsson, “State-space models for stored energy and  $q$ -  
 factors,” in *Electromagnetic Theory (EMTS), 2016 URSI Inter-  
 national Symposium on* (IEEE, 2016) pp. 226–228.

<sup>5</sup>D. Seetharamdoo, *Étude des métamatériaux à indice de réfrac-  
 tion négatif: paramètres effectifs et applications antennaires po-  
 tentielles*, Ph.D. thesis, Rennes 1 (2006).

<sup>6</sup>L. D. Landau, J. Bell, M. Kearsley, L. Pitaevskii, E. Lifshitz, and  
 J. Sykes, *Electrodynamics of continuous media*, Vol. 8 (elsevier  
 2013).

<sup>7</sup>I. Semchenko, A. Balmakou, S. Khakhomov, and S. Tretyakov,  
 “Stored and absorbed energy of fields in lossy chiral single-  
 component metamaterials,” Physical Review B **97**, 014432  
 (2018).

<sup>8</sup>S. Tretyakov, “Electromagnetic field energy density in artificial  
 microwave materials with strong dispersion and loss,” physics  
 Letters A **343**, 231–237 (2005).

<sup>9</sup>M. H. Rabah and D. Seetharamdoo, “Calculation of the total  $q$ -  
 factor for electrically small antennas with metamaterials using  
 characteristic modes,” in *2016 10th European Conference on An-  
 tennas and Propagation (EuCAP)* (IEEE, 2016) pp. 1–5.

<sup>10</sup>R. W. Ziolkowski, “Applications of metamaterials to realize effi-  
 cient electrically small antennas,” in *Antenna Technology: Small  
 Antennas and Novel Metamaterials, 2005. IWAT 2005. IEEE  
 International Workshop on* (IEEE, 2005) pp. 7–10.

<sup>11</sup>D. Sarkar, S. M. Mikki, A. M. Alzahed, K. V. Srivastava, and  
 Y. M. Antar, “New considerations on electromagnetic energy in  
 antenna near-field by time-domain approach,” in *2017 IEEE Ap-  
 plied Electromagnetics Conference (AEMC)* (IEEE, 2017) pp. 540  
 1–2.

<sup>12</sup>G. W. Hanson and A. B. Yakovlev, *Operator theory for electro-  
 magnetics: an introduction* (Springer Science & Business Media,  
 2013).

<sup>13</sup>W. C. Gibson, *The method of moments in electromagnetic*  
 (Chapman and Hall/CRC, 2007).

<sup>14</sup>M. Cabedo-Fabres, E. Antonino-Daviu, A. Valero-Nogueira, and  
 M. F. Bataller, “The theory of characteristic modes revisited: A  
 contribution to the design of antennas for modern applications,”  
 IEEE Antennas and Propagation Magazine **49**, 52–68 (2007).

<sup>15</sup>Y. Chen and C.-F. Wang, *Characteristic modes: Theory and ap-  
 plications in antenna engineering* (John Wiley & Sons, 2015).

<sup>16</sup>Y. Chen and C.-F. Wang, “Hf band shipboard antenna design  
 using characteristic modes,” IEEE Transactions on Antennas and  
 Propagation **63**, 1004–1013 (2015).

<sup>17</sup>S. Genovesi, F. A. Dicandia, and A. Monorchio, “Excitation of  
 multiple characteristic modes on a three dimensional platform,”

in *2017 11th European Conference on Antennas and Propagation  
 (EUCAP)* (IEEE, 2017) pp. 1769–1771.

<sup>18</sup>D.-W. Kim and S. Nam, “Systematic design of a multiport mimo  
 antenna with bilateral symmetry based on characteristic mode  
 analysis,” IEEE Transactions on Antennas and Propagation **66**,  
 1076–1085 (2017).

<sup>19</sup>M. H. Rabah, D. Seetharamdoo, M. Berbineau, and A. De Lus-  
 trac, “New metrics for artificial magnetism from metal-dielectric  
 metamaterial based on the theory of characteristic modes,” IEEE  
 Antennas and Wireless Propagation Letters **15**, 460–463 (2016).

<sup>20</sup>M. Capek, P. Hazdra, and J. Eichler, “A method for the evalua-  
 tion of radiation  $q$  based on modal approach,” IEEE Transactions  
 on Antennas and Propagation **60**, 4556–4567 (2012).

<sup>21</sup>M. H. Rabah, D. Seetharamdoo, and M. Berbineau, “Analysis of  
 miniature metamaterial and magnetodielectric arbitrary-shaped  
 patch antennas using characteristic modes: Evaluation of the  $q$   
 factor,” IEEE Transactions on Antennas and Propagation **64**,  
 2719–2731 (2016).

<sup>22</sup>J. Eichler, P. Hazdra, M. Capek, and M. Mazanek, “Modal  
 resonant frequencies and radiation quality factors of microstrip  
 antennas,” International Journal of Antennas and Propagation  
**2012** (2012).

<sup>23</sup>R. Martens, E. Safin, and D. Manteuffel, “Inductive and capaci-  
 tive excitation of the characteristic modes of small terminals,” in  
*2011 Loughborough Antennas & Propagation Conference* (IEEE,  
 2011) pp. 1–4.

<sup>24</sup>D. Seetharamdoo, M.-h. Rabah, H. Srour, and M. Berbineau,  
 “Method for improving the efficiency of an electrically small an-  
 tenna,” (2019), uS Patent App. 16/311,474.

<sup>25</sup>M. Cabedo Fabres, *Systematic design of antennas using the the-  
 ory of characteristic modes*, Ph.D. thesis (2008).

<sup>26</sup>M. H. Rabah, *Design methodology of antennas based on meta-  
 materials and the theory of characteristic modes: application to  
 cognitive radio*, Ph.D. thesis, Lille 1 (2015).

<sup>27</sup>M. H. Rabah and D. Seetharamdoo, “Analysis and design of meta-  
 material structures using the theory of characteristic modes,” in  
*2017 11th European Conference on Antennas and Propagation  
 (EUCAP)* (IEEE, 2017) pp. 2676–2680.

<sup>28</sup>R. Garbacza and D. Pozar, “Antenna shape synthesis using char-  
 acteristic modes,” IEEE Transactions on Antennas and Propaga-  
 tion **30**, 340–350 (1982).

<sup>29</sup>M. M. Elsewe and D. Chatterjee, “Characteristic mode analysis  
 of microstrip patch shapes,” in *2017 IEEE International Sym-  
 posium on Antennas and Propagation & USNC/URSI National  
 Radio Science Meeting* (IEEE, 2017) pp. 2107–2108.

<sup>30</sup>B. Yang and J. J. Adams, “Systematic shape optimization of sym-  
 metric mimo antennas using characteristic modes,” IEEE Trans-  
 actions on Antennas and Propagation **64**, 2668–2678 (2015).

<sup>31</sup>E. FEKO, “Simulation software,” (2014).

<sup>32</sup>R. Harrington and J. Mautz, “Theory of characteristic modes for  
 conducting bodies,” IEEE Transactions on Antennas and Propa-  
 gation **19**, 622–628 (1971).

<sup>33</sup>M. C. Fabres, “Systematic design of antennas using the theory  
 of characteristic modes,” Universidad Politecnica Valencia , 118–  
 120 (2007).

<sup>34</sup>R. Harrington and T.-H. E. Fields, “Hoboken,” (2001).

<sup>35</sup>M. Gustafsson, J. Friden, and D. Colombi, “Antenna current op-  
 timization for lossy media with near-field constraints,” IEEE An-  
 tennas and Wireless Propagation Letters **14**, 1538–1541 (2014).

<sup>36</sup>M. Cismasu and M. Gustafsson, “Antenna bandwidth optimiza-  
 tion with single frequency simulation,” IEEE Transactions on  
 Antennas and Propagation **62**, 1304–1311 (2013).

<sup>37</sup>W. Geyi, “A method for the evaluation of small antenna  $q$ ,”  
 IEEE Transactions on Antennas and Propagation **51**, 2124–2129  
 (2003).

<sup>38</sup>H. Benosman and N. B. Hacene, “Design and simulation of double  
 s” shaped metamaterial,” International Journal of Computer  
 Science Issues (IJCSI) **9**, 534 (2012).

<sup>39</sup>X. Chen, T. M. Grzegorzczak, B.-I. Wu, J. Pacheco Jr, and  
 J. A. Kong, “Robust method to retrieve the constitutive effective  
 parameters of metamaterials,” Physical Review E **70**, 016608  
 (2004).

- <sup>40</sup>D. Smith, D. Vier, T. Koschny, and C. Soukoulis, “Electromagnetic parameter retrieval from inhomogeneous metamaterials,” *Physical review E* **71**, 036617 (2005).
- <sup>560</sup> <sup>41</sup>A. Sihvola, “Metamaterials in electromagnetics,” *Metamaterials* **1**, 2–11 (2007).
- <sup>565</sup> <sup>42</sup>Y. Rahmat-Samii, “Metamaterials in antenna applications: Classifications, designs and applications,” in *Antenna Technology Small Antennas and Novel Metamaterials, 2006 IEEE International Workshop on* (IEEE, 2006) pp. 1–4. **585**
- <sup>43</sup>H. Chen, J. Zhang, Y. Bai, Y. Luo, L. Ran, Q. Jiang, and J. A. Kong, “Experimental retrieval of the effective parameters of metamaterials based on a waveguide method,” *Optics Express* **14**, 12944–12949 (2006).
- <sup>570</sup> <sup>44</sup>X. Chen, B.-I. Wu, J. A. Kong, and T. M. Grzegorzczak, “Retrieval of the effective constitutive parameters of bianisotropic metamaterials,” *Physical Review E* **71**, 046610 (2005).
- <sup>575</sup> <sup>45</sup>D. Seetharamdoo, R. Sauleau, K. Mahdjoubi, and A.-C. Tarot, “Effective parameters of resonant negative refractive index metamaterials: Interpretation and validity,” *Journal of applied physics* **98**, 063505 (2005).
- <sup>46</sup>R. O. Ouedraogo, E. J. Rothwell, A. R. Diaz, K. Fuchi, and A. Temme, “Miniaturization of patch antennas using a metamaterial-inspired technique,” *IEEE Transactions on Antennas and Propagation* **60**, 2175–2182 (2012).
- <sup>47</sup>A. Erentok and R. W. Ziolkowski, “Metamaterial-inspired efficient electrically small antennas,” *IEEE Transactions on Antennas and Propagation* **56**, 691–707 (2008).
- <sup>48</sup>P. Jin and R. W. Ziolkowski, “Metamaterial-inspired, electrically small huygens sources,” *IEEE Antennas and Wireless Propagation Letters* **9**, 501–505 (2010).
- <sup>49</sup>J. L. Ethier, *Antenna shape synthesis using characteristic mode concepts*, Ph.D. thesis, Université d’Ottawa/University of Ottawa (2012).
- <sup>50</sup>S. Kasap and P. Capper, *Springer handbook of electronic and photonic materials* (Springer, 2017).
- <sup>51</sup>K. Schab, L. Jelinek, M. Capek, C. Ehrenborg, D. Tayli, G. A. Vandenbosch, and M. Gustafsson, “Energy stored by radiating systems,” *IEEE Access* **6**, 10553–10568 (2018).
- <sup>52</sup>D. Nyberg, P.-S. Kildal, and J. Carlsson, “Radiation Q and radiation efficiency of wideband small antennas and their relation to bandwidth and cut-off of spherical modes,” (2007).